Identification, pathological, and genomic characterization of novel goose reovirus associated with liver necrosis in geese, China

Xinyu Zhang,[*,1] Gaojie Chen,[*,1] Runzhi Liu,[*] Jinyue Guo,[*] Kun Mei,[*] Limei Qin,[*] Zhili Li,[*] Sheng Yuan,[*] Shujian Huang,[*,†] and Feng Wen ®[*,‡,2]

[*]College of Life Science and Engineering, Foshan University, Foshan 528231, Guangdong, China; [†]Guangdong Huasheng Biotechnology Co., Ltd，Guangzhou 511300, Guangdong, China; and [‡]Guangdong Provincial Key Laboratory of Animal Molecular Design and Precise Breeding, College of Life Science and Engineering, Foshan University, Foshan 528231, Guangdong, China

ABSTRACT Since 2021, a novel strain of goose reovirus (**GRV**) has emerged within the goose farming industry in Guangdong province, China. This particular viral variant is distinguished by the presence of white necrotic foci primarily localized in the liver and spleen, leading to substantial economic losses for the poultry industry. However, the etiology, prevalence and genomic characteristics of the causative agent have not been thoroughly investigated. In this study, we conducted an epidemiological inquiry employing suspected GRV samples collected from May 2021 to September 2022. The macroscopic pathological and histopathological lesions associated with GRV-infected clinical specimens were examined. Moreover, we successfully isolated the GRV strain and elucidated the complete genome sequence of the isolate GD21/88. Through phylogenetic and recombination analysis, we unveiled that the GRV strains represent a novel variant resulting from multiple reassortment events. Specifically, the μNS, λC, and σNS genes of GRV were found to have originated from chicken reovirus, while the σA gene of GRV exhibited a higher degree of similarity with a novel duck reovirus. The remaining genes of GRV were traced back to Muscovy duck reovirus. Collectively, our findings underscore the significance of GRV as a pathogenic agent impacting the goose farming industry. The insights gleaned from this study contribute to a more comprehensive understanding of the epidemiology of GRV in Southern China and shed light on the genetic reassortment events exhibited by the virus.

Key words: reovirus, goose reovirus, Muscovy duck reovirus, avian reoviruses, σC

INTRODUCTION

Avian reoviruses (**ARVs**), members of the *Orthoreovirus* genus within the *Reovirales* order, exhibit a wide distribution among poultry and wild birds worldwide. These versatile pathogens are capable of infecting various avian species, including chickens, ducks, turkeys, ostriches, geese, pigeons, and parrots (Sánchez-Cordón et al., 2002; Sakai et al., 2009; Styś-Fijoł et al., 2017; Czekaj et al., 2018). The impact of ARVs on the poultry industry is substantial, leading to significant economic losses. The initial isolation of ARVs can be traced back to 1954, when these viruses were identified in chickens displaying symptoms of viral arthritis and growth impairment (Fahey and Crawley, 1954). Subsequently, in 1972, Muscovy duck reovirus (**MDRV**) was discovered in Muscovy ducklings, presenting yellowish-white or white necrotic foci within the liver (Gaudry et al., 1972). Since 2006, a novel strain of duck reovirus, designated as NDRV, has been responsible for outbreaks of spleen hemorrhage and necrosis in Peking ducklings in China (Liu et al., 2011; Zhu et al., 2015; Zheng et al., 2016). Additionally, the first documented case of goose reovirus (**GRV**) emerged in 2003, causing acute inflammation of the spleen and liver, followed by subacute or chronic viral arthritis, tenosynovitis, and pericarditis in geese (Palya et al., 2003). Genotype analysis has revealed that MDRV and GRV belong to genotype 1, while NDRV was classified under genotype 2 (Wang et al., 2013).

Since July 2020, an emerging GRV infection presenting with liver and spleen white focal necrosis has swiftly disseminated across goose farms in Guangdong, China, resulting in a mortality rate of 10 to 20% (Huang et al.,

2022; Zhang et al., 2023). It has been suggested that this novel GRV variant shares close genetic relatedness to MDRV (He et al., 2022). This outbreak of GRV stands as a significant infectious disease, posing a considerable threat to China's goose industry. Furthermore, investigations have revealed that coinfection of the closely related duck reovirus and *Salmonella Indiana* dramatically escalates mortality rates among ducklings (Wang et al., 2020), suggesting a substantial risk of coinfection with GRV for duck goslings.

The genome of GRV comprises 10 segments of double-stranded RNA, which can be classified into 3 groups based on their fragment size: L, M, and S. L1-L3 encode 3 structural proteins, namely λA, λB, and λC, respectively. M1-M3 encode 2 structural proteins, μA and μB, as well as a nonstructural protein, μNS. S1 to S3 not only encode 2 structural proteins, σA and σB, but also express a nonstructural protein, σNS. S4 expresses the structural protein σC and additionally generates the p10 protein through multiple sense and antisense transcription (Benavente and Martínez-Costas, 2007). The viral capsid is composed of σC, σB, and μB, while the inner core is constituted by σB, λA, λB, λC, and μA. Notably, the σC protein interacts with α-2,3-sialyllactose, α-2,6-sialyllactose, or α-2,8-di-siallylactose on host cells, facilitating viral entry and determining the *orthoreovirus* serotype (Reiter et al., 2011). The p10 protein, known as the fusion-associated small transmembrane (**FAST**) protein, exhibits an asymmetric membrane topology, featuring a relatively small N-terminal extracellular domain and a C-terminal cytoplasmic domain. The C-terminal cytoplasmic tails of the FAST protein promote membrane fusion and facilitate syncytium formation (Barry and Duncan, 2009). Studies employing the *Reovirales* reverse genetic system have demonstrated that the FAST protein enhances virus rescue efficiency through this mechanism; however, excessive FAST protein can impede virus replication (Kanai et al., 2017; Kanai and Kobayashi, 2021).

In this study, we have successfully isolated a novel strain of GRV associated with liver and spleen white focal necrosis in geese from Guangdong, China. Subsequent pathological and genetic characterization of this novel GRV variant has been conducted.

MATERIALS AND METHODS

Clinical Investigations, Tissue RNA Extraction, and cDNA Synthesis

From May 2021 to September 2022, a total of 114 suspected GRV infected samples characterized by white necrotic foci on liver tissues were collected from 39 distinct goose farms located in the Guangdong province, China. To confirm the presence of GRV infection, 0.5 g of liver, spleen, and pancreas tissue samples were homogenized in 1 mL of phosphate-buffered solution (**PBS**) with a pH of 7.4. The resulting supernatant underwent 2 successive cycles of freezing and thawing at $-80°$C. Subsequently, total RNA was extracted using the Trizol reagent (Thermo Fisher Scientific, MA) following the manufacturer's guidelines. The extracted RNA was then utilized for cDNA synthesis using the HiScript III 1st Strand cDNA Synthesis Kit (Vazyme, Nanjing, China), following the manufacturer's protocol.

GRV Detection

A set of primers (GRV-F: 5′-AGGATACAGTGTTC-CATCCTG-3′, GRV-R: 5′-ACTGGATCCAGAGTG-CAGAAT-3′) was designed using Primer Premier 5.0 software and synthesized by Sangon Biotech (Shanghai, China) Co., Ltd. These primers were specifically designed to detect the presence of GRV based on the conserved regions in the σC gene, with an expected amplification product size of 333 bp. The PCR reaction mixture consisted of 10 μL of 2× Taq Plus Master Mix II (Vazyme, Nanjing, China), 1.5 μL of cDNA, 1 μL each of 10 μM GRV-F and GRV-R primers, and 9 μL of BeyoPure Ultrapure Water (Beyotime, Shanghai, China). The PCR amplification was carried out with the following cycling parameters: initial denaturation at 95°C for 3 min, denaturation at 95°C for 15 s, annealing at 55°C for 30 s, and extension at 72°C for 30 s, with a total of 35 cycles; final extension at 72°C for 5 min, followed by temporary storage at 4°C. The PCR products were separated by electrophoresis on a 2% agarose (Thermo Fisher Scientific, MA) gel at 120 V for 45 min, and the results were visualized using a gel imaging instrument.

Virus Isolation and Validation

Liver tissues obtained from GRV-positive samples were homogenized in sterile PBS (pH = 7.4) supplemented with 200 U/mL penicillin (Beyotime, Shanghai, China) and 0.2 mg/mL streptomycin (Beyotime, Shanghai, China). The resulting homogenate was frozen at $-80°$C, thawed at room temperature, and this process was repeated twice. Subsequently, it was centrifuged at 12,000 × g for 5 min. The resulting homogenate underwent 3 cycles of freezing and thawing, followed by centrifugation at 12,000 × g for 5 min. The supernatant was collected and filtered through a 0.22 μm Supor Membrane Acrodisc Syringe Filter (Jet, Guangdong, China). The filtered supernatant was then incubated on chicken embryo fibroblast cells (DF-1, ATCC CRL-12203) for 2 h, and subsequently supplemented with minimum essential medium (**MEM**) (Gibco, Grand Island) for further incubation of 72 h at 37°C with 5% CO_2. The resulting viral solution was collected and stored at $-80°$C. The GD21/88 strain was obtained after 3 consecutive passages. DF-1 cells were cultured at 37°C with 5% CO_2 in an incubator using Dulbecco's modified Eagle medium (**DMEM**) (Gibco, Grand Island) supplemented with 10% fetal bovine serum (**FBS**) (Gibco, Grand Island), 100 U/mL penicillin (Beyotime, Shanghai, China), and 0.1 mg/mL streptomycin (Beyotime, Shanghai, China). The viral solution obtained as described above was inoculated into either 9- to 11-day-old specific-pathogen-free (**SPF**) embryonated chicken eggs or 12- to 15-

day-old goose eggs via the allantoic cavity, and then incubated at 37°C for 72 to 96 h. The allantoic fluid was collected and stored at −80°C until further use. Viral RNA was extracted from the cell culture supernatant and allantoic fluid using the AxyPrepTM Body Fluid Viral DNA/ RNA Miniprep Kit (Axygen, Hangzhou, China). The extracted RNA was used to synthesize cDNA with the HiScript III 1st Strand cDNA Synthesis Kit (Vazyme, Nanjing, China) according to the manufacturer's instructions. The presence of GRV was validated by the PCR assay described above.

Histopathology Analysis

The tissue samples were stored at −80°C to maintain their integrity and prevent degradation. Based on the clinical signs, autopsy, and PCR screening results, a subset of GRV positive liver tissues were fixed with 4% paraformaldehyde fix solution (Beyotime, Shanghai, China) for further histopathological analysis. The fix solution was changed every 12 h until the fixative was clarified. Samples were embedded in paraffin, and hematoxylin-eosin (**HE**) staining was performed as previously described (Liang et al., 2022).

Complete Genome Sequencing

Complete genome sequences of GD21/88 were amplified with primers (Table 1) designed based on the goose reovirus sequences available in the GenBank. The Phusion Hot Start II High-Fidelity PCR Master Mix (Thermo Fisher Scientific, MA) was used to amplify the whole genome segments. The cDNA of the above GRV positive samples (GD21/88, GD22/412, GD22/435,

GD22/721, GD22/776, GD22/817, GD22/818) were amplified using a 50 μL reaction system with the following components: 2× High-Fidelity PCR Master Mix 25 μL, cDNA 3 μL, 10 μM upstream and downstream primers 2 μL each, and BeyoPure Ultrapure Water (DNase/RNase-Free, Sterile) (Beyotime, Shanghai, China) 18 μL. The 2-step PCR reaction procedure was as follows: 4 cycles of predenaturation for 3 min at 95°C, denaturation for 15 s at 95°C, annealing for 30 s at 45°C, extension at 72°C for 2 min, followed by 31 cycles of denaturation for 15 s at 95°C, annealing for 30 s at 50°C to 65°C, extension at 72°C for 2 min, and finally 72°C extension for 10 min. All 10 gene segments of GD21/88 were successfully ligated to pMD 18-T Vector Cloning Kit (TaKaRa, Dalian, China), and the viral sequences were determined by Sanger sequencing. The sequence assembly was performed using the SeqMan program (DNASTAR, Madison,).

Sequence Analysis

The open reading frames (**ORFs**) of GRV were predicted utilizing the DNASTAR Lasergene 12 software suite (DNASTAR, Inc.). Subsequently, a phylogenetic analysis was conducted for the GRV σC gene, given its significance as a genetic marker for distinguishing and classifying orthoreovirus isolates. A total of 40 representative avian orthoreovirus virus sequences were extracted from the GenBank database. These sequences were aligned using the MAFFT program, integrated within the UGENE software (Version 36.0). The UGENE software (Version 36.0) was further employed to generate the distance matrix for the σC genes. The seqlogos of σC protein was constructed by an online Blast2logo program using PSI-blast. Employing MEGA software (Version 7.0), an exemplary maximum likelihood phylogenetic tree was constructed, incorporating the 7 acquired sequences of GRV σC alongside representative strains of GRV, MDRV, and NDRV sourced from the GenBank database. This construction was performed with 1,000 bootstrap replicates to ensure robustness and reliability.

Recombination Detection

The whole genome sequence of GD21/88 was analyzed for recombination with MDRV (ZJ2000M) (Yun et al., 2013), NDRV (091) (Ma et al., 2012), and chicken reovirus (**CRV**) (S1133) (Supplementary Table 1) (Bodelón et al., 2001). The recombination events of L, M, and S segments of the *orthoreovirus* in this study were screened using the Recombination Detection Program (**RDP**) as previously described (Wen et al., 2021). The recombination was confirmed significant when the recombination signal was supported by at least 2 methods, and $p \leq 0.05$ was considered statistically significant. Similarity plot analysis (Simplot version 3.5.1) was used to visualize the possible recombination sites of representative strains.

Table 1. Primers used for viral sequencing.

Primers	Primer sequences (5′−3′)	Product size (bp)
GRV-S4-F	GCTTTTTCCTTCTCCTTAGTGGTC	1124
GRV-S4-R	GATGAATAGCCCTTCCCCG	
GRV-S3-F	GCTTTTTGAGTCCTTGTGCAG	1191
GRV-S3-R	GATGAGTAAGAGTCCAAGTCGTG	
GRV-S2-F	ATGGAGGTACGTGTGCCAAAC	1124
GRV-S2-R	CTACCAACCACACTCAATGA	
GRV-S1-F	ATGGCGCGTGCCGTGTACGACTT	1251
GRV-S1-R	CTAGACGGTAAAAGTGGCTAGTA	
GRV-M3-F	GCTTTTTGAGTCCTAGCGTGGA	1997
GRV-M3-R	GATGAATAACTGAGTCTGCCGT	
GRV-M2-F	ATGGGCAACGCTACGTCTGT	2029
GRV-M2-F	TCACGAAGGCTTAAAGAA	
GRV-M1-F	GCTTTTCTCGACATGGCCTATC	2283
GRV-M1-R	GATGAATATCTCAAGACGGCTAAC	
GRV-L3-F	GCTTTTTCACCCATGGCTCAG	1943
GRV-L3-1943R	TTATTGGAGACAAGCGGCTTCAT	
GRV-L3-1921F	ATGAAGCCGCTTGTCTCCAATAA	1987
GRV-L3-R	GATGAGTAACACCCTTCTACTGGAG	
GRV-L2-F	GCTTTTTCCTCACCATGCGAGT	1973
GRV-L2-1973R	AAGTTTCGCTAACCATTGGCA	
GRV-L2-1974F	TATCAGCGTGGTTTTGAGTATCAGG	1857
GRV-L2-R	GATGAGTAATTCCTCGAGCCATG	
GRV-L1-F	GCTTTTTCTCCGAACGCCGAAAT	2015
GRV-L1-2015R	TARCCGACCATRGCATTAGCC	
GRV-L1-1995F	GGCTAATGCYATGGTCGGYTA	1965
GRV-L1-R	GATGAATAACCTCCAACGAGAGTC	

Table 2. Epidemiological survey of GRV from May 2021 to September 2022.

Time	Total samples	Positive sample	Positive rate (%)
5/2021-8/2021	22	9	40.91
9/2021-12/2021	14	3	21.43
1/2022-4/2022	66	8	12.12
5/2022-9/2022	12	6	50.00
Total	114	26	22.81

the Chou-Fasman and Garnier-Robson methods were utilized to analyze the α-helical and β-sheet regions within the σC protein, respectively. For the prediction of flexible regions, the Karplus-Schultz algorithm was employed, while the Kyte-Doolittle approach was employed to assess the hydrophilicity of the protein. To further investigate the epitopes and antigenic potential, the Emini and Jameson-Wolf methods were employed, respectively.

RESULTS

Clinical Investigation

From May 2021 to September 2022, a total of 114 suspected cases of GRV were collected and subjected to PCR identification, resulting in the screening of 26 GRV-positive samples (Table 2). The cases were predominantly observed in meat geese, adult geese, and breeder geese between 15 and 40 d of age, with a higher likelihood of occurrence in environments characterized by poor growth conditions and high humidity. The disease exhibited a year-round prevalence, with a higher incidence during cold and rainy seasons. Clinically, affected geese displayed symptoms such as fever, loose feathers, emaciation, white watery feces, and difficulty in walking, often accompanied by limping and reduced mobility.

Gross Pathology and Histopathology

During postmortem examination of geese, significant histopathological changes were observed in the infected organs and tissues. Hemorrhage was observed in the myocardium (Figure 1D), and the spleen exhibited enlargement (Figure 1C). Notably, large, focal, white, needle-tip-sized lesions were observed in the spleen and liver (Figure 1A−C). Microscopic examination following HE staining revealed extensive hepatocyte degeneration and necrosis (Figure 2A), accompanied by inflammatory cell infiltration, chromatin margination, and the presence of crescent-shaped clusters or irregular aggregates (Figure 2B). Furthermore, muscle cells surrounding the liver blood vessels displayed edema and rupture (Figure 2C).
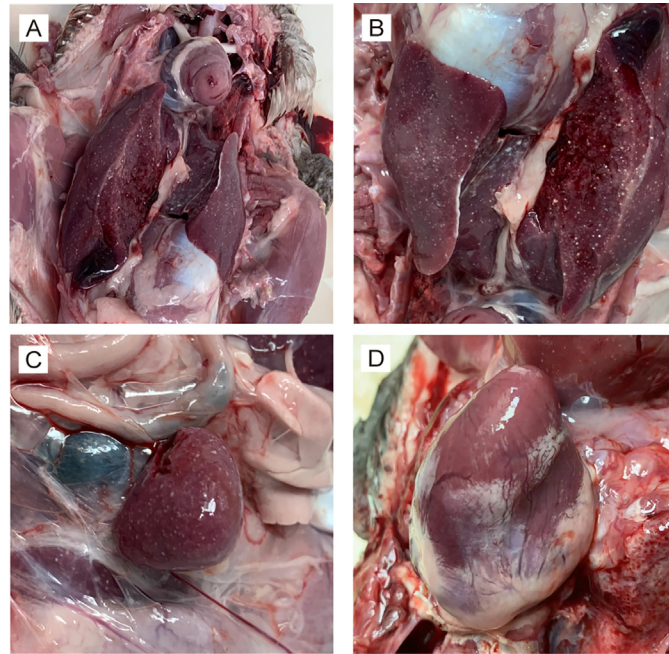

Figure 1. Gross lesions of goose infected with goose reovirus (GRV). Photographs were taken of Magang geese at around 40 d of age on a goose farm. (A) Macroscopic thoracic anatomical alterations in geese. (B) Localized hepatic lesions characterized by whitish discoloration in geese. (C) Markedly enlarged spleen, accompanied by minuscule white focal lesions. (D) Cardiac hemorrhage and elevated adipose tissue deposition on the cardiac surface.

Prediction of Secondary Structure and B-Cell Antigenic Epitopes of σC Protein

The algorithms incorporated in the DNA Star Lasergene software (Version, 7.1.0) were employed to forecast the secondary conformation of the protein. Specifically,

Figure 2. Histopathological lesions in the liver tissue of geese infected by GRV as observed through HE staining. (A) Microscopic examination of the liver tissue at a magnification of 100× reveals histological abnormalities. (B) Focal lesions exhibit noticeable infiltration of inflammatory cells, accompanied by hemorrhage, hepatocyte lysis, and necrosis upon closer inspection. (C) Edematous fractures in the muscle cells of the hepatic vessel wall.
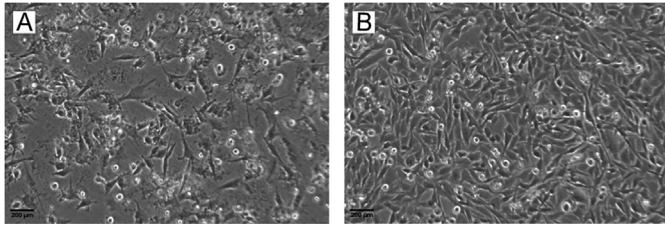
Figure 3. Cellular morphology of DF-1 cells 48 h post-GRV infection (100×). (A) Morphology of infected cells. (B) Morphology of control group cells.

Isolation of GRV

In this study, the GRV was isolated after 3 passages of goose liver tissue homogenate in DF-1 cells. Following inoculation of DF-1 cells with GD21/88, cytopathic effects were observed within 24 h. After 48 h of GRV infection, 80% of the DF-1 cells displayed cytopathic effects including cell lysis, cell fusion, and boundary disappearance (Figure 3). The presence of GRV in the cell culture was confirmed by conventional RT-PCR, and the virus was designated as Reo/Goose/Guangdong/88/2021 (GD21/88).

Complete Genome Sequence of GRV

Among the positive samples, 7 (GD21/88, GD22/412, GD22/435, GD22/721, GD22/776, GD22/817, GD22/818) were selected for sequencing of the S4 gene. The complete genome sequences of GD21/88 (GenBank accession number: OR890071-OR890080) were successfully obtained using RT-PCR with a set of designed primers. The genome length of the GD21/88 strain in this study was 22,675 bp. The sizes of the 10 gene segments were as follows: S4 (1,124 bp), S3 (1,191 bp), S2 (1,104 bp), S1 (1,251 bp), M3 (1,997 bp), M2 (2,029 bp), M1 (2,283 bp), L3 (3,907 bp), L2 (3,830 bp), and L1 (3,959 bp). Predicted ORFs analysis showed that, except for the S4 segment which encodes 2 proteins (p10 and σC), all other segments were single-stranded and encoded a single protein (λA, λB, λC, μA, μB, μNS, σA, σB, and σNS).

Phylogenetic Tree and Sequence Analysis

As is well known, σC is commonly used as a genetic marker to differentiate and classify *Orthoreovirus*. The results of the phylogenetic analysis demonstrated that the downloaded representative 45 σC sequences exhibited 3 distinct branches of ARVs. Specifically, 21 sequences were classified within the first branch, 12 sequences within the second branch, and 7 sequences within the third branch (Figure 4). All 7 GRV strains investigated in this study were in the first branch, which was mainly composed of MDRV and included the GRV isolated from geese in 2020. Within the first branch, the GRV strains isolated in 2020 and thereafter formed a new subgroup (Figure 4), to which all 7 GRV strains investigated in this study belonged.

The σC sequences of GD21/88 and GD22/776 were found to be highly similar to the 2020 GRV strains, while GD22/721, GD22/817, and GD22/818 displayed genetic variations (Figure 5). A comparison of the amino acid sequences of these 7 viruses with 10 other GRV sequences in the first branch revealed that GD21/88 and GD22/776 were identical (Supplementary Table 2), while differing from GD22/721, GD22/817, and GD22/818 by 5 amino acids (L32F, Q53R, Y56H, W140R, and S265F). GD21/88 differed from GD22/412 and GD22/435 by 4 amino acids (H161D, N213D, R260Q, A267V). Interestingly, these 7 amino acid sequences shared a common amino acid site difference (V6A) with other GRV sequences. Amino acid sequences within the GRV branch exhibited amino acid mutation sites that differed from other GRV sequences, including E3G, P5L, Y10C, S14F, D21G, S51L, M70V, E79K, D83G, A89T, C93R, A94G, T95V, H97L, N108T, V113T, T191A, P203L, D223E, S239D, and S241A (Supplementary Figure 1).

Secondary Structure and B-Cell Antigenic Epitopes of σC Protein

The coding region of the σC protein is composed of 810 nucleotides, encoding 269 amino acids, with a molecular weight of 29383.6 and a theoretical isoelectric point (**PI**) of 6.49. Serine (**Ser**) is the most abundant amino acid in the σC protein, accounting for 15.24%, followed by leucine (**Leu**) at 11.15%. The number of acidic amino acid residues is 25, the number of charged amino acid residues is 62, and the number of hydrophobic amino acids (AILFWV) is 105, accounting for 39.03%. According to Kyte-Doolittle, the average total hydrophobicity index of the σC protein is −0.16. The flexible regions primarily occur at amino acids 5-9, 13-26, 36-55, 76-86, 109-111, 117-118, 124-131, 138-140, 165-168, 171-175, 181-184, 190-208, 222-229, 233-237, and 252-256. The antigenic regions are mainly found at amino acids 1-9, 14-27, 36-56, 62-70, 77-96, 99-102, 107-110, 118-120, 145-147, 163-166, 173-175, 190-208, 220-230, 234-239, and 252-258. The regions with a higher probability on the surface are primarily located at amino acids 18-23, 44-49, 52-55, 163-167, 197-205, 223-229, and 252-257. In general, amino acid fragments contained within the hydrophobic region, flexible region, and antigenic region are likely to be B-cell epitopes, including amino acids 18-23, 44-49, 52-55, 197-205, 223-229, and 252-256 (Figure 6).

Recombination Analysis

Recombination events between the GD21/88 strain and other representative strains such as S1133-CRV, ZJ2000M-MDRV, and 091-DRV were evaluated (Figure 7). The similarity plot analysis results suggested that the μNS, λC, and σNS genes of GD21/88 were more similar to S1133-CRV. The σA gene of GD21/88 exhibited higher similarity with 091-NDRV. However, the remaining gene segments of GD21/88 displayed higher similarity with ZJ2000M-MDRV. These findings
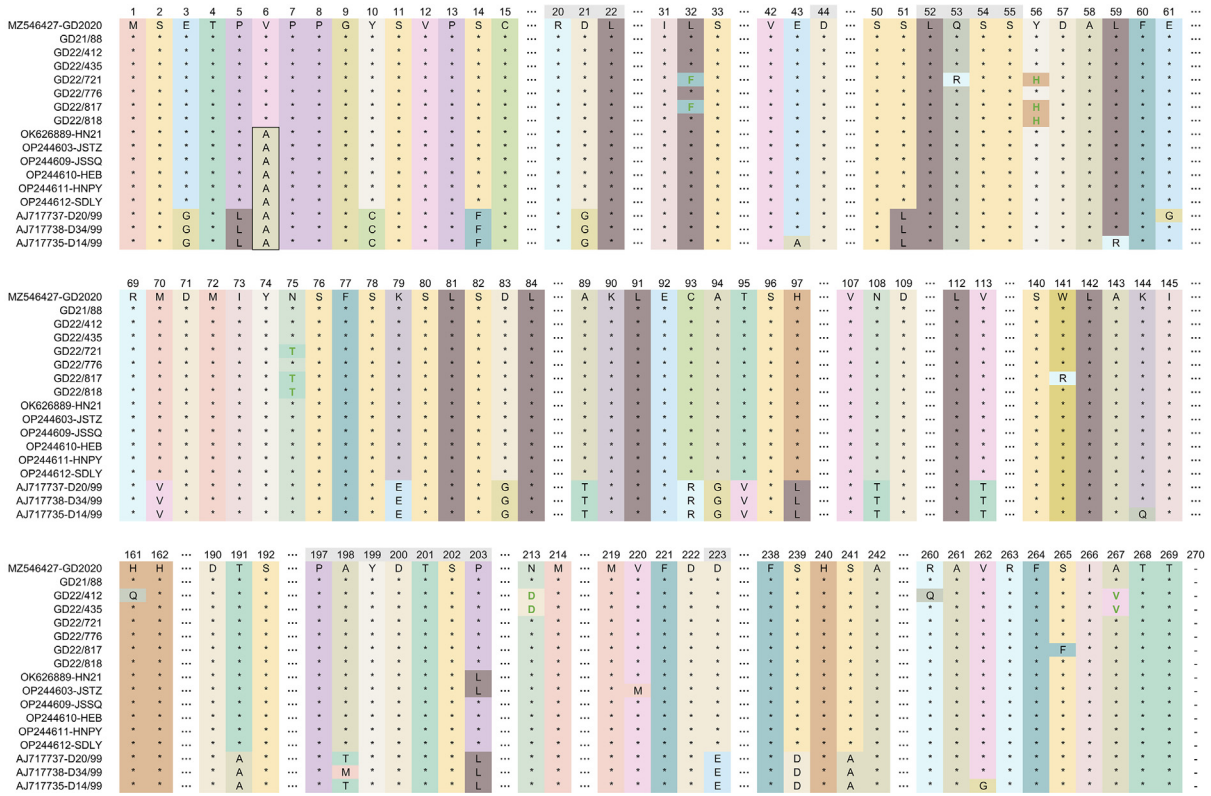
Figure 4. Construction of phylogenetic trees based on avian reovirus σC genes using the neighbor-joining method in the MEGA5.10 program. Bootstrap percentages obtained after 1,000 replicates are indicated at nodes. GD21/88 is denoted by a green triangle, while GD22/721, GD22/776, GD22/817, and GD22/818 are denoted by gray triangles.

indicate that the novel GRV is a reassortant that originated from CRV, NDRV, and MDRV (Figure 8).

DISCUSSION

Since 2021, an infectious ailment characterized by the occurrence of focal necrotic white lesions in the liver and spleen of goose has emerged in Guangdong Province, leading to substantial economic losses in China's waterfowl farming sector. A novel variant strain of the avian *orthoreovirus*, specifically identified as GRV GD2020, has been isolated and recognized from the deceased geese's liver and spleen (Huang et al., 2022). From May 2021 to September 2022, a total of 114 samples were screened using PCR, resulting in the identification of 26 samples testing positive for GRV. In our investigation, a high seroprevalence of GRV was observed among geese in Guangdong, China. Furthermore, the positivity rate exhibited an upward trajectory from the second quarter of 2021 to the second quarter of 2022, indicating the

widespread presence of GRV in Guangdong and its significance as a pathogen in the goose farming industry. Among the positive samples (GD21/88, GD22/412, GD22/435, GD22/721, GD22/776, GD22/817, GD22/818), 7 were chosen for sequencing of the S4 gene, all of which exhibited substantial similarity to GRV GD2020. Through full genome sequencing, GD21/88 was found to bear a strong resemblance to GRV GD2020 and belonged to a new variant strain of the avian *orthoreovirus*.

The σC protein possesses the ability to induce cellular apoptosis (Shih et al., 2004) and plays a pivotal role in binding to cellular receptors and triggering specific neutralizing antibodies (Wickramasinghe et al., 1993; Guardado Calvo et al., 2005). Simultaneously, the σC gene exhibits evolutionary trends in its genetic sequence, making it a commonly employed genetic marker for distinguishing avian *orthoreoviruses* (Liu et al., 2003). Sequence analysis of the 7 strains revealed them all to be GRV, with an increasing number of mutation sites appearing over time. Notably, when comparing GRV

Figure 5. Amino acid sequence comparison of σC protein. The number of each individual amino acid sequence is provided on the left. The position of each amino acid in the protein sequence is indicated above the sequence. Identical amino acids to the reference sequence are denoted by (*). Gray shading represents predicted B-cell epitopes. The boxed black lines indicate sites where goose reovirus (GRV) differs from other goose-derived Muscovy duck reoviruses.

with other goose-origin MDRV mutation sites, attention should be directed toward 3 sites, namely D21G, P203L, and D223E, all situated within the predicted B-cell epitopes. Additionally, recent alterations in amino acid sites of the GRV σC protein were detected, including Q53R, which is located within the predicted B-cell epitope. The

impact of these mutations on alterations in host adaptability and immune responses remains unexplored. One of the vital mechanisms underlying the evolution of segmented viruses is the recombination of genome fragments (Ayalew et al., 2020). Phylogenetic and recombination analyses revealed that GD21/88 may
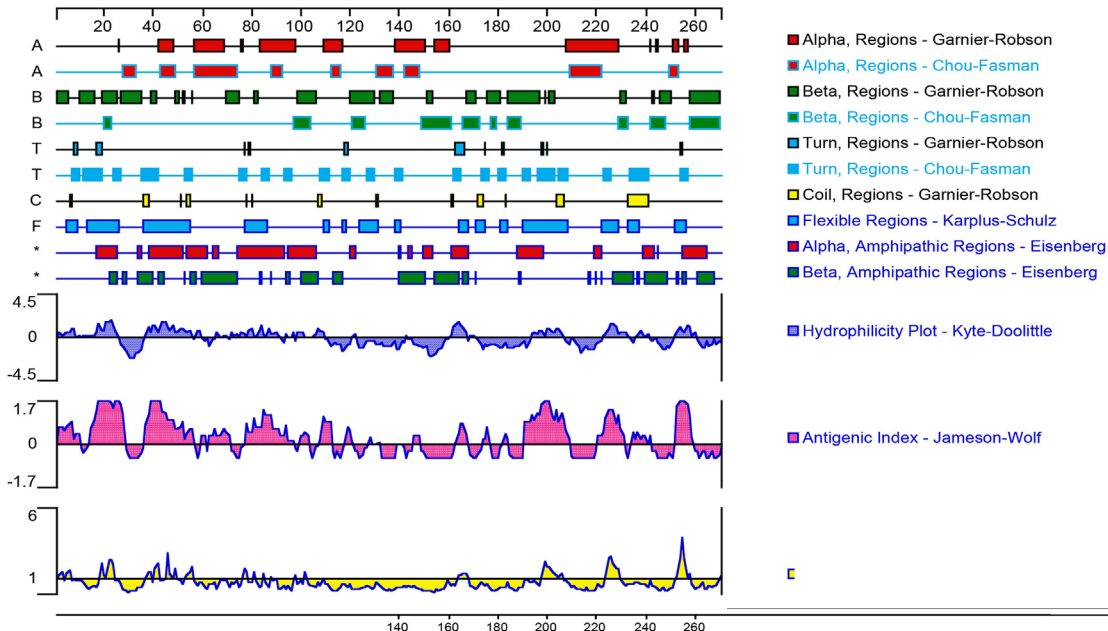
Figure 6. Analyses of hydrophilicity, flexible regions, antigenic index, and surface probability of the goose reovirus σC protein. Protein secondary structure prediction was performed using the modules provided by DNA Star Lasergene Protean software (Version, 7.1.0).
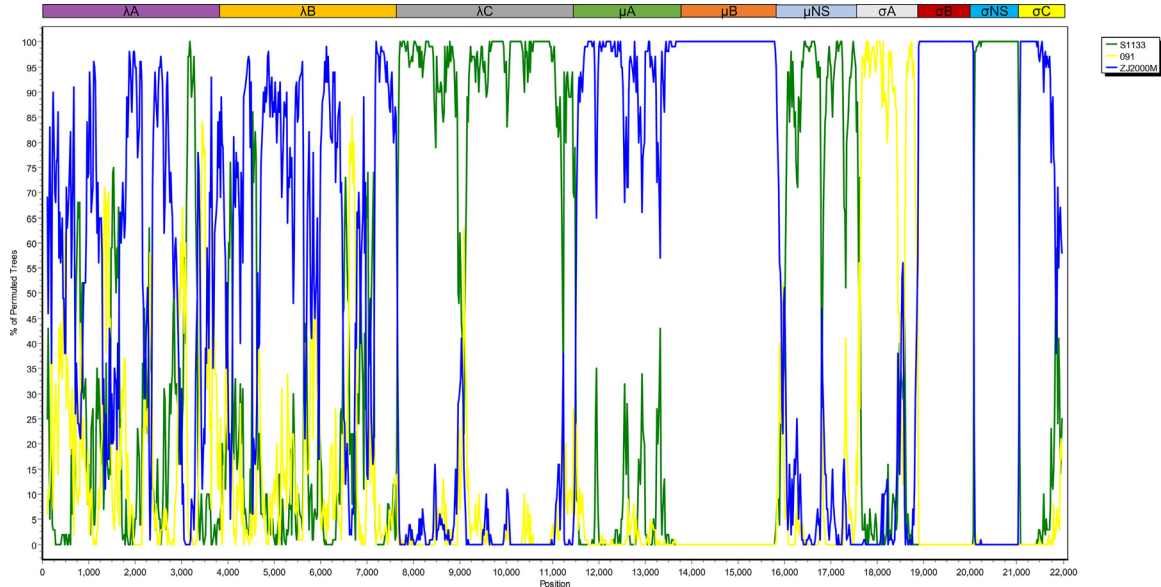
Figure 7. Genome-wide recombination analysis of GD21/88. Simplot 3.5.1 was employed to conduct recombinant analysis on the gene fragments of λ, μ, and σ proteins from GD21/88. The GD21/88 gene served as the query sequence, while S1133—chicken reovirus (green), 091—novel duck reovirus (yellow), and ZJ2000M—Muscovy duck reovirus (orange) were utilized as representative parents for similarity map analysis. The GenBank accession numbers corresponding to the sequences used in this analysis are provided in Table S1.

represent a triple-recombinant strain, with genetic contributions from CRV, DRV, and MDRV, with σA originating from DRV and λC, μNS, and σNS originating from CRV. Further investigations are warranted to delve into this matter in future studies.

In conclusion, we successfully cloned and analyzed the complete genome sequence of a mutant strain of GRV, and identified the σC gene in an additional 6 GRV strains, thereby confirming their classification as a novel variant of MDRV. Phylogenetic and recombination analyses unveiled GRV as a triple-recombinant virus, though additional research is necessary to validate this finding. Our study contributes valuable information to the ARV database, thus providing a theoretical foundation for further comprehension of the evolutionary relationships and cross-species transmission of GRV in relation to other ARVs. These findings hold significant implications for the prevention and control of GRV outbreaks within the goose industry.
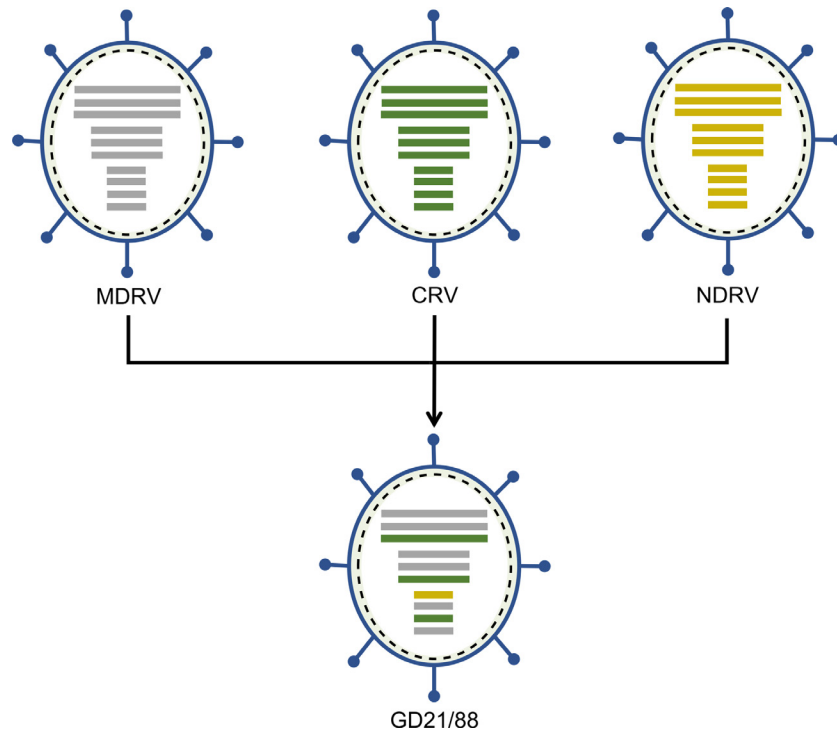

Figure 8. Schematic diagram of GD21/88 genome-wide recombination results. The Muscovy duck reovirus (MDRV) gene is indicated in gray, the chicken reovirus (CRV) gene in green, and the novel duck reovirus (NDRV) gene in yellow. GD21/88 is a triple-derived recombinant strain, in which μNS, λNS, and σNS originated with chicken reovirus, the gene of σA was derived from duck reovirus, and the rest of genes were provided by MDRV.

ACKNOWLEDGMENTS

Data Availability Statement: The datasets used and/or analyzed during the current study are available from the corresponding author on reasonable request.

DISCLOSURES

The authors declare that they have no competing interests.

SUPPLEMENTARY MATERIALS

Supplementary material associated with this article can be found in the online version at doi:10.1016/j.psj.2023.103269.

REFERENCES

Ayalew, L. E., K. A. Ahmed, Z. H. Mekuria, B. Lockerbie, S. Popowich, S. K. Tikoo, D. Ojkic, and S. Gomis. 2020. The dynamics of molecular evolution of emerging avian reoviruses through accumulation of point mutations and genetic re-assortment. Virus Evol. 6:veaa025.

Barry, C., and R. Duncan. 2009. Multifaceted sequence-dependent and -independent roles for reovirus FAST protein cytoplasmic tails in fusion pore formation and syncytiogenesis. J. Virol. 83:12185–12195.

Benavente, J., and J. Martínez-Costas. 2007. Avian reovirus: structure and biology. Virus Res. 123:105–119.

Bodelón, G., L. Labrada, J. Martínez-Costas, and J. Benavente. 2001. The avian reovirus genome segment S1 is a functionally tricistronic gene that expresses one structural and two nonstructural proteins in infected cells. Virology 290:181–191.

Czekaj, H., W. Kozdruń, N. Styś-Fijoł, J. S. Niczyporuk, and K. Piekarska. 2018. Occurrence of reovirus (ARV) infections in poultry flocks in Poland in 2010-2017. J. Vet. Res. 62:421–426.

Fahey, J. E., and J. F. Crawley. 1954. Studies on chronic respiratory disease of chickens II. Isolation of a virus. Can. J. Comp. Med. Vet. Sci. 18:13–21.

Gaudry, D., J. M. Charles, and J. Tektoff. 1972. A new disease expressing itself by a viral pericarditis in Barbary ducks. C. R. Acad. Hebd. Seances Acad. Sci. D 274:2916–2919.

Guardado Calvo, P., G. C. Fox, X. L. Hermo Parrado, A. L. Llamas-Saiz, C. Costas, J. Martínez-Costas, J. Benavente, and M. J. van Raaij. 2005. Structure of the carboxy-terminal receptor-binding domain of avian reovirus fibre sigmaC. J. Mol. Biol. 354:137–149.

He, D., F. Wang, L. Zhao, X. Jiang, S. Zhang, F. Wei, B. Wu, Y. Wang, Y. Diao, and Y. Tang. 2022. Epidemiological investigation of infectious diseases in geese on mainland China during 2018-2021. Transbound. Emerg. Dis. 69:3419–3432.

Huang, Y., J. Zhang, J. Dong, L. Li, R. Kuang, M. Sun, and M. Liao. 2022. Isolation and characterization of a new goose orthoreovirus causing liver and spleen focal necrosis in geese, China. Transbound. Emerg. Dis. 69:3028–3034.

Kanai, Y., and T. Kobayashi. 2021. FAST proteins: development and use of reverse genetics systems for reoviridae viruses. Annu. Rev. Virol. 8:515–536.

Kanai, Y., S. Komoto, T. Kawagishi, R. Nouda, N. Nagasawa, M. Onishi, Y. Matsuura, K. Taniguchi, and T. Kobayashi. 2017. Entirely plasmid-based reverse genetics system for rotaviruses. Proc. Natl. Acad. Sci. U. S. A. 114:2349–2354.

Liang, Z., J. Guo, S. Yuan, Q. Cheng, X. Zhang, Z. Liu, C. Wang, Z. Li, B. Hou, S. Huang, and F. Wen. 2022. Pathological and molecular characterization of a duck plague outbreak in Southern China in 2021. Animals 12:3523.

Liu, H. J., L. H. Lee, H. W. Hsu, L. C. Kuo, and M. H. Liao. 2003. Molecular evolution of avian reovirus: evidence for genetic diversity and reassortment of the S-class genome segments and multiple cocirculating lineages. Virology 314:336–349.

Liu, Q., G. Zhang, Y. Huang, G. Ren, L. Chen, J. Gao, D. Zhang, B. Han, W. Su, J. Zhao, X. Hu, and J. Su. 2011. Isolation and characterization of a reovirus causing spleen necrosis in Pekin ducklings. Vet. Microbiol. 148:200–206.

Ma, G., D. Wang, J. Shi, T. Jiang, Y. Yuan, and D. Zhang. 2012. Complete genomic sequence of a reovirus isolate from Pekin ducklings in China. J. Virol. 86:13137.

Palya, V., R. Glávits, M. Dobos-Kovács, E. Ivanics, E. Nagy, K. Bányai, G. Reuter, G. Szucs, A. Dán, and M. Benko. 2003. Reovirus identified as cause of disease in young geese. Avian Pathol. 32:129–138.

Reiter, D. M., J. M. Frierson, E. E. Halvorson, T. Kobayashi, T. S. Dermody, and T. Stehle. 2011. Crystal structure of reovirus attachment protein $\sigma1$ in complex with sialylated oligosaccharides. PLoS Pathog. 7:e1002166.

Sakai, K., Y. Ueno, S. Ueda, K. Yada, S. Fukushi, M. Saijo, I. Kurane, K. Mutoh, K. Yoshioka, M. Nakamura, K. Takehara, S. Morikawa, and T. Mizutani. 2009. Novel reovirus isolation from an Ostrich (Struthio camelus) in Japan. Vet. Microbiol. 134:227–232.

Sánchez-Cordón, P. J., J. Hervás, F. Chacón de Lara, J. Jahn, F. J. Salguero, and J. C. Gómez-Villamandos. 2002. Reovirus infection in psittacine birds (Psittacus erithacus): morphologic and immunohistochemical study. Avian Dis. 46:485–492.

Shih, W. L., H. W. Hsu, M. H. Liao, L. H. Lee, and H. J. Liu. 2004. Avian reovirus sigmaC protein induces apoptosis in cultured cells. Virology 321:65–74.

Styś-Fijoł, N., W. Kozdruń, and H. Czekaj. 2017. Detection of avian reoviruses in wild birds in Poland. J. Vet. Res. 61:239–245.

Wang, W., J. Liang, M. Shi, G. Chen, Y. Huang, Y. Zhang, Z. Zhao, M. Wang, M. Li, M. Mo, T. Wei, T. Huang, X. He, and P. Wei. 2020. The diagnosis and successful replication of a clinical case of duck spleen necrosis disease: an experimental co-infection of an emerging unique reovirus and Salmonella Indiana reveals the roles of each of the pathogens. Vet. Microbiol. 246:108723.

Wang, D., J. Shi, Y. Yuan, L. Zheng, and D. Zhang. 2013. Complete sequence of a reovirus associated with necrotic focus formation in the liver and spleen of Muscovy ducklings. Vet. Microbiol. 166:109–122.

Wen, F., J. Yang, A. Li, Z. Gong, L. Yang, Q. Cheng, C. Wang, M. Zhao, S. Yuan, Y. Chen, S. El-Ashram, Y. Li, H. Yu, J. Guo, and S. Huang. 2021. Genetic characterization and phylogenetic analysis of porcine epidemic diarrhea virus in Guangdong, China, between 2018 and 2019. PLoS One 16:e0253622.

Wickramasinghe, R., J. Meanger, C. E. Enriquez, and G. E. Wilcox. 1993. Avian reovirus proteins associated with neutralization of virus infectivity. Virology 194:688–696.

Yun, T., B. Yu, Z. Ni, W. Ye, L. Chen, J. Hua, and C. Zhang. 2013. Isolation and genomic characterization of a classical Muscovy duck reovirus isolated in Zhejiang, China. Infect. Genet. Evol. 20:444–453.

Zhang, S., X. Wang, Y. Diao, and Y. Tang. 2023. Recombinant characteristics, pathogenicity, and transmissibility of a variant goose orthoreovirus derived from inter-lineage recombination. Vet. Microbiol. 277:109620.

Zheng, X., D. Wang, K. Ning, T. Liang, M. Wang, M. Jiang, and D. Zhang. 2016. A duck reovirus variant with a unique deletion in the sigma C gene exhibiting high pathogenicity in Pekin ducklings. Virus Res. 215:37–41.

Zhu, Y. Q., C. F. Li, Z. L. Bi, Z. Y. Chen, C. C. Meng, G. J. Wang, C. Ding, and G. Q. Liu. 2015. Molecular characterization of a novel reovirus isolated from Pekin ducklings in China. Arch. Virol. 160:365–369.